Supporting Information for

Near-infrared and metal-free tetra(butylamino)phthalocyanine nanoparticles for dual modal cancer phototherapy

Ying-Jie Wu,‡[a] Fan-Hong Lv, ‡[a] Jing-Lan Kan,*[a] Qun Guan,[a] Anqi Xue,[b] Quanbo Wang,[b] Yan-An Li,[a] and Yu-Bin Dong*[a]

[a] College of Chemistry, Chemical Engineering and Materials Science, Collaborative Innovation Center of Functionalized Probes for Chemical Imaging in Universities of Shandong, Key Laboratory of Molecular and Nano Probes, Ministry of Education, Shandong Normal University, Jinan 250014, P. R. China.

[b] Shandong Analysis and Test Center, Qilu University of Technology (Shandong Academy of Sciences), Jinan 250014, P. R. China.

* Corresponding authors.

E-mail addresses: kanjinglan@163.com (J.-L. Kan), yubindong@sdnu.edu.cn (Y.-B. Dong).

‡ Contributed equally

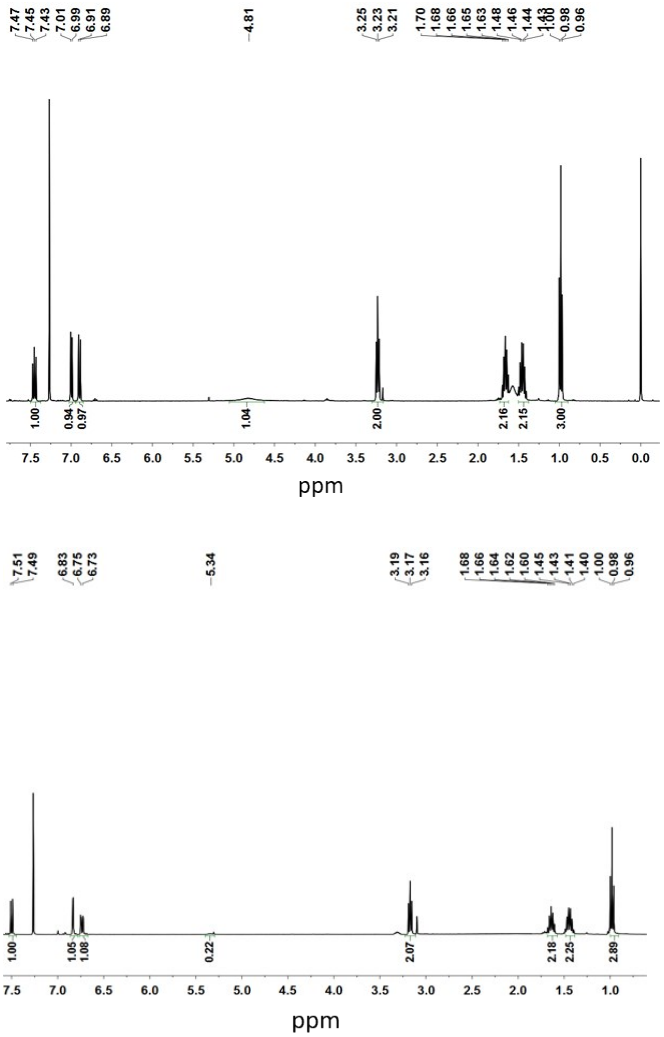

Fig. S1 ^{1}H NMR spectra of 3-butylaminophthalonitrile (top) and 4-butylaminophthalonitrile (bottom) in $CDCl_3$. The signal at 7.26 ppm was attributed to the residual $CHCl_3$.

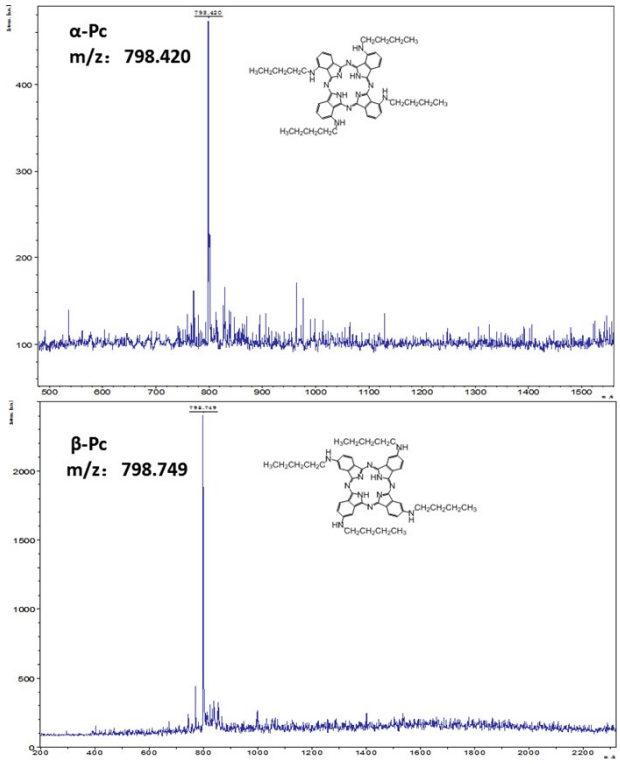

Fig. S2 MALDI-TOF mass spectra for ***α*-Pc** and ***β*-Pc**.

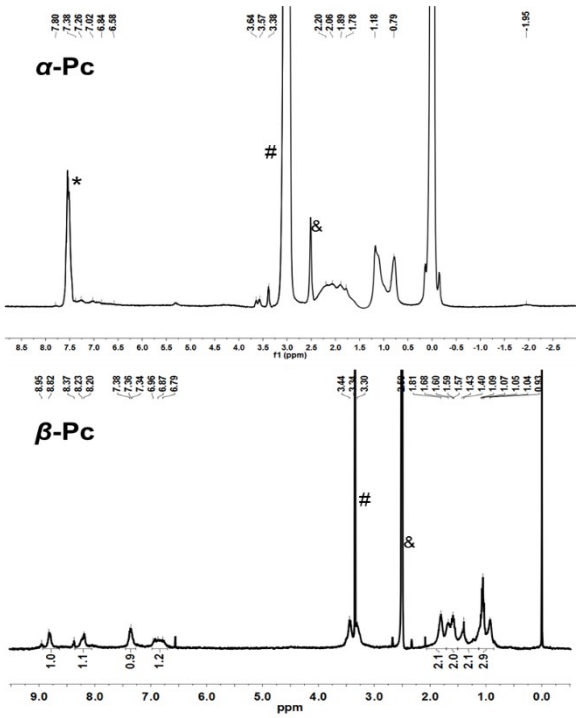

Fig. S3 ^{1}H NMR spectra of ***α*-Pc** (top) in $CDCl_3$/[D_6]DMSO (6:1) and ***β*-Pc** (bottom) in [D_6]DMSO (with the signals due to residues of $CHCl_3$, H_2O and DMSO denoted as *,$^{\#}$ and $^{\&}$, respectively).

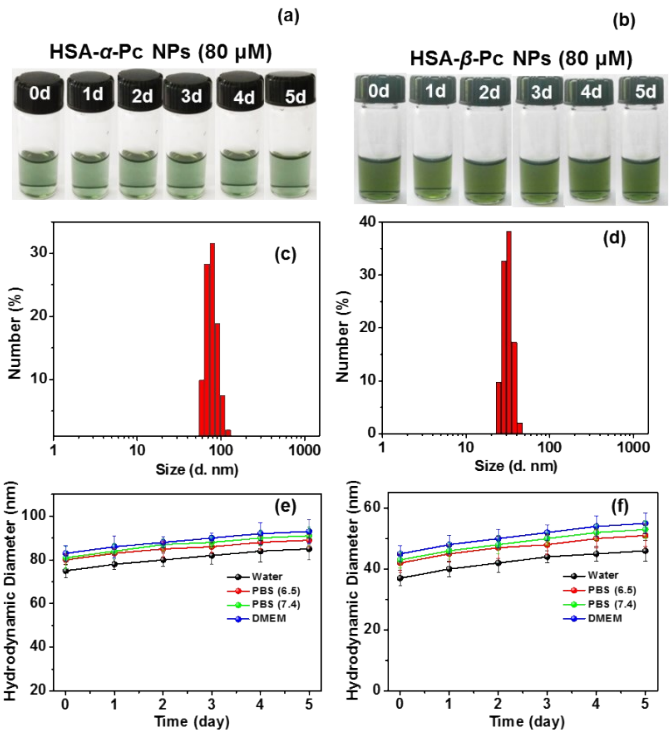

Fig. S4 Pictures of **HSA-*α*-Pc** NP (a) and **HSA-*β*-Pc** NP (b) in water (both at 80 μM, Pc equiv) after standing for different time. The DLS analysis of **HSA-*α*-Pc** NP (c) and **HSA-*β*-Pc** NP (d) dispersed in aqueous solution. The DLS stability of **HSA-*α*-Pc** NP (e) and **HSA-*β*-Pc** NP (f) in various media for five days, and the data were based on the results of 3 independent experiments.

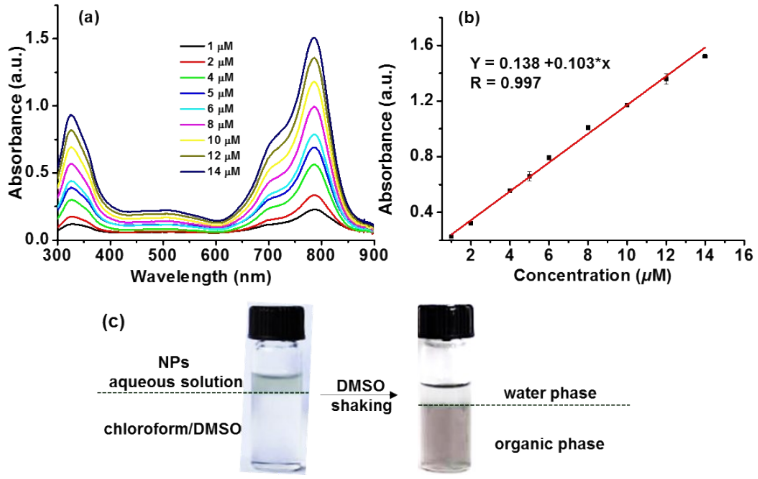

Fig. S5 (a) The UV-vis spectra of ***α*-Pc** in V($CHCl_3$) :V(DMSO) = 95:5 solution at different concentrations. (b) The calibration curve of ***α*-Pc** at 786 nm. The absorbance data were presented as mean ± SD (*n* = 3). (c) The procedure of calculating the amounts of ***α*-Pc** in NP aqueous solution by using organic solvent extraction.

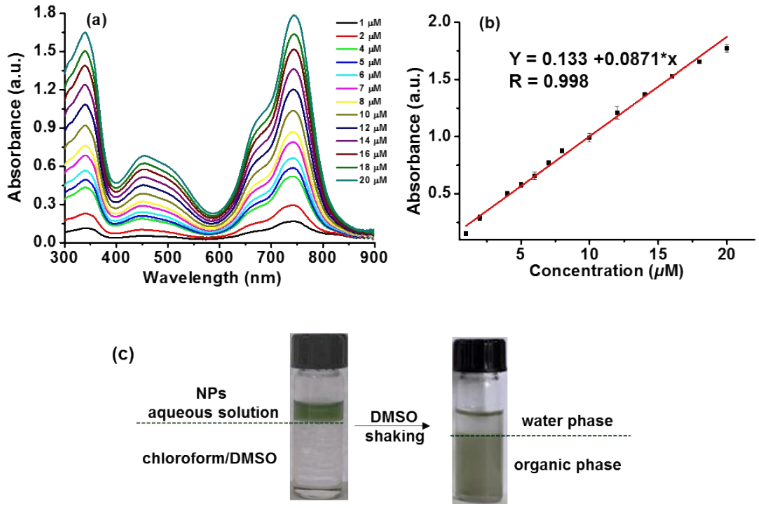

Fig. S6 (a) The UV-vis spectra of ***β*-Pc** in V($CHCl_3$) : V(DMSO) = 95:5 solution at different concentrations. (b) The calibration curve of ***β*-Pc** at 742 nm. The absorbance data were presented as mean ± SD (*n* = 3). (c) The procedure of calculating the amounts of ***β*-Pc** in NP aqueous solution by using organic solvent extraction.

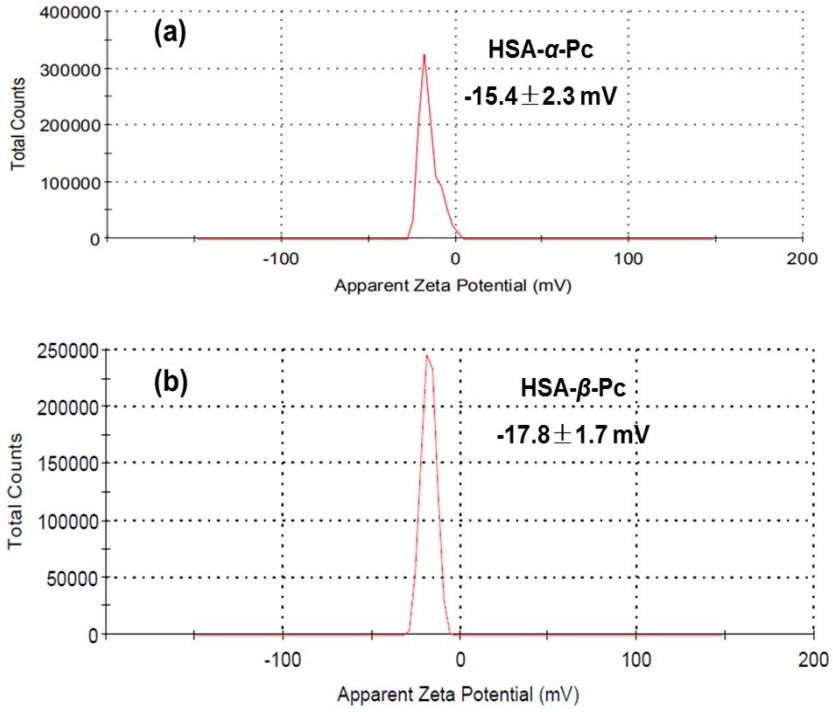

Fig. S7 The zeta potentials of **HSA-*α*-Pc** NP (a) and **HSA-*β*-Pc** NP (b) in water solution at 25°C (both at 80 μM, Pc equiv).

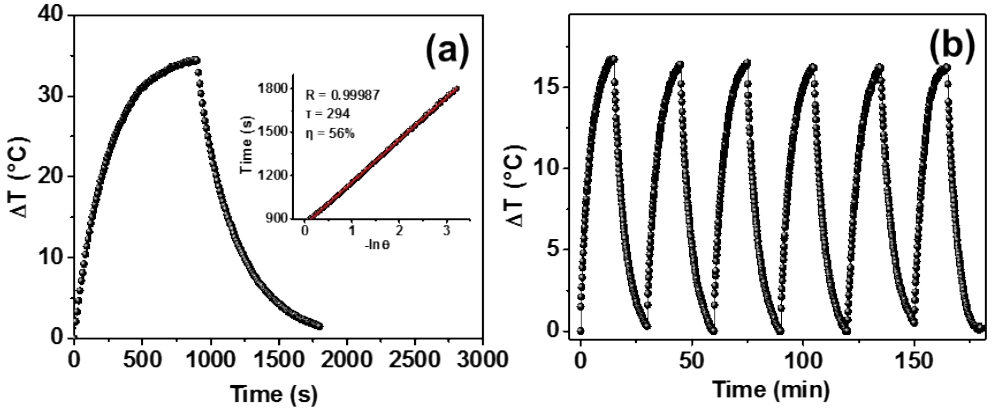

Fig. S8 Photothermal property of **HSA-*α*-Pc** NP in aqueous solution under 808 nm laser irradiation. (a) Photothermal effect and the laser was switched off after irradiation for 15 min (80 μM Pc equiv, 1.5 W·cm^{-2}). The inset presents the plot of cooling time (15 min) *vs* the negative natural logarithm of the temperature driving force obtained from the cooling stage. (b) Temperature variations for 6 cycles of the (1.5 W·cm^{-2}, 15 min per cycle) at the concentration 20 μM (Pc equiv).

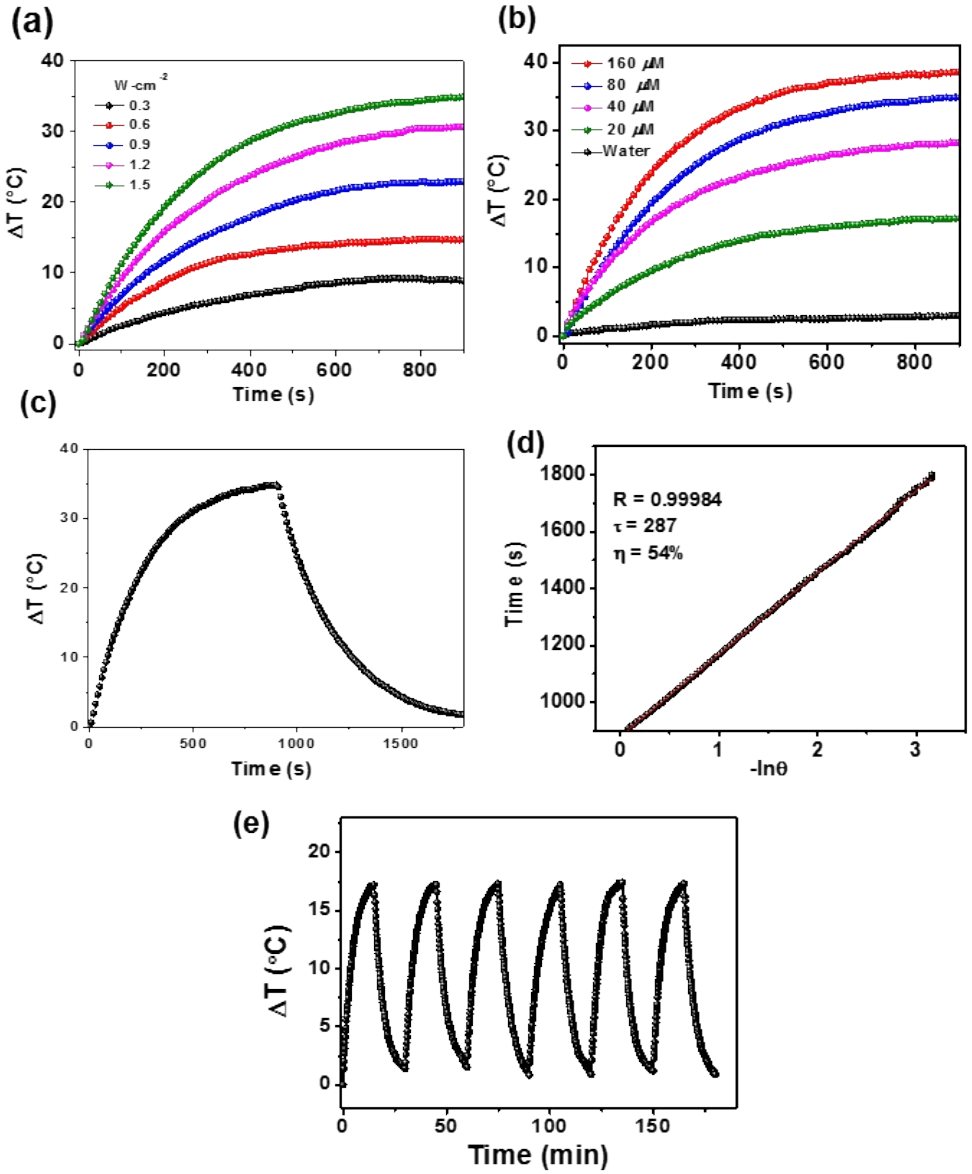

Fig. S9 Photothermal property of **HSA-*β*-Pc** NP dispersed in water under 808 nm laser irradiation. (a) Temperature elevation in dependence of light intensity at the concentration of 80 μM (Pc equiv). (b) Concentration-dependent temperature elevation with an intensity of 0.9 W·cm^{-2}. (c) Photothermal effect and the laser was switched off after irradiation for 15 min (80 μM, Pc equiv., 1.5 W·cm^{-2}). (d) Plot of cooling time (15 min) *vs* the negative natural logarithm of the temperature driving force obtained from the cooling stage. (e) Temperature variations for 6 cycles of the (1.5 W·cm^{-2}, 15 min per cycle) at the concentration 20 μM (Pc equiv).

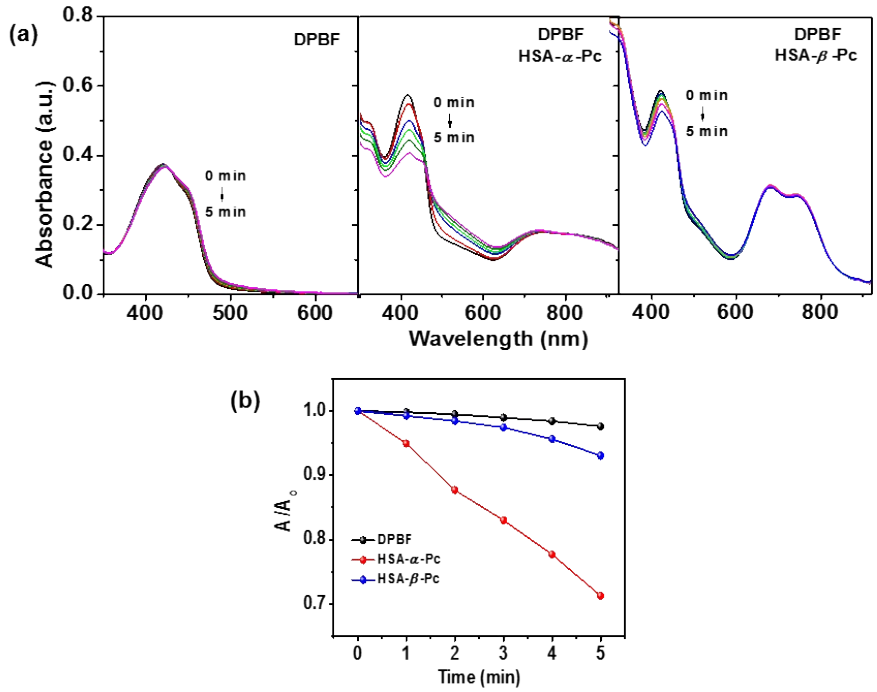

Fig. S10 Singlet oxygen generation ability of the **HSA-*α*-Pc** and **HSA-*β*-Pc** NPs. (a) Time-dependent UV-vis absorption of DPBF/DMF (1.33 mM, 62 μL) at 420 nm with **HSA-*α*-Pc** and **HSA-*β*-Pc** (both at 20 μM Pc equiv, 2.0 mL) in aqueous solution under 808 nm laser irradiation (1.5 W·cm^{-2}) for 5 min. (b) Comparison of the decay rate of DPBF, **HSA-*α*-Pc** and **HSA-*β*-Pc**.

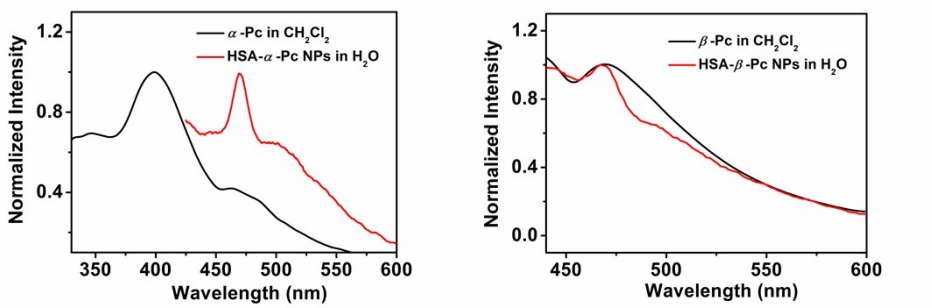

Fig. S11 Fluorescence spectra of ***α*-Pc** (5 μM, CH_2Cl_2, excited at 300 nm) and ***β*-Pc** (5 μM, CH_2Cl_2, excited at 309 nm) as well as **HSA-*α*-Pc** and **HSA-*β*-Pc** NPs (both at 20 μM, Pc equiv) in water upon irradiated at 405 nm.

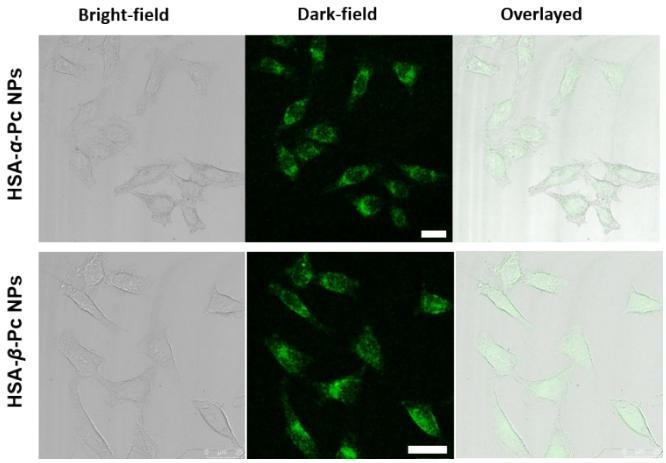

Fig. S12 *In vitro* CLSM images of MCF-7 cells treated with **HSA-*α*-Pc** and **HSA-*β*-Pc** NPs (both at 20 μM, Pc equiv) for 2 h, using a green channel for phthalocyanine (λ_{ex} = 405 nm, 440-480 nm), scale bar 25 μm.

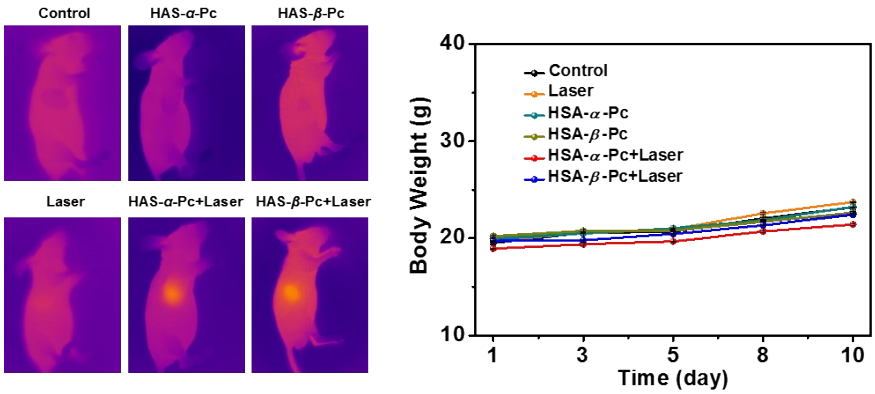

Fig. S13 (Left) Thermal imageries of the nude mice. (Right) Body weight of the mice in various groups during the treatment. The data are presented as the mean ± SD (n = 4).

Table S1. ^{1}H NMR spectroscopic data (δ) for 3-butylaminophthalonitrile, 4-butylaminophthalonitrile, ***α*-Pc** and ***β*-Pc**.

Compound (Solvent)	**δ**
3-butylaminophthalonitrile ($CDCl_3$)	7.47-7.43 (t, 1H,-C_6H_3-), 7.01-6.99 (d, 1H,-C_6H_3-), 6.91-6.89 (d, 1H, -C_6H_3-), 4.81 (s, 1H, -NH-), 3.25-3.21 (t, 2H, -CH_2-), 1.70-1.63 (m, 2H, -CH_2-), 1.48-1.43 (m, 2H, -CH_2-), 1.00-0.96 (t, 3H, -CH_3)
4-butylaminophthalonitrile ($CDCl_3$)	7.51-7.49 (d, 1H,-C_6H_3-), 6.83 (s, 1H,-C_6H_3-), 6.75-6.73 (d, 1H, -C_6H_3-), 5.34 (s, 1H, -NH-), 3.19-3.16 (t, 2H, -CH_2-), 1.68-1.60 (m, 2H, -CH_2-), 1.45-1.40 (m, 2H, -CH_2-), 1.00-0.96 (t, 3H, -CH_3).
***α*-Pc** ($CDCl_3$/[D_6]DMSO (6:1))	7.80-6.58 (-Pc_{C6H3}-), 3.64-3.38 (4H, -NH-), 2.20-1.78 (-CH_2-), 1.18-0.79 (-$CH_2CH_2CH_3$), -1.95 (-Pc_{NH}-).
***β*-Pc** ([D_6]DMSO)	8.95-8.82 (4H, -Pc_{C6H3}-), 8.37-8.20 (4H, -Pc_{C6H3}-), 7.38-7.34 (4H, -Pc_{C6H3}-), 6.96-6.79 (4H, -NH-), 3.44-3.30 (-NH$\underline{CH_2}$-), 1.81-0.93 (28H, -$CH_2CH_2CH_3$).

Table S2. Summary of recent typical Pc-nanomaterials for PTT/PDT synergistic phototherapy in living cells by a single light source.

sample	light source ($W \cdot cm^{-2}$)	η (%)	PS (μM)	MTT (%)	ref.
Pc@HSNs	730 nm (1.5)	37	~575	30	1
NanoPcTB	655 nm (2.5)	--	6	20	2
ZnPc NW	808 nm (3.0)	--	~205	50	3
O_2@PFH@$HMoS_x$-HSA/AlPc	670 nm (1.0)	40	~255	25	4
GR-TSCuPc	650 nm (3.0)	--	~15	40	5

SWNHs−TSCuPc	650 nm (3.0)	--	~15	15	6
ZnPc NPs	650 nm (0.7)	31	20	~15	7
HSA-*β*-Pc	808 nm (1.5)	54	20	31	this work
HSA-*α*-Pc	808 nm (1.5)	56	20	20	this work

References

1. J. Peng, L. Zhao, X. Zhu, Y. Sun, W. Feng, Y. Gao, L. Wang and F. Li, *Biomaterials*, 2013, **34**, 7905-7912.
2. X. Li, C. Y. Kim, S. Lee, D. Lee, H. M. Chung, G. Kim, S. H. Heo, C. Kim, K. S. Hong and J. Yoon, *J. Am. Chem. Soc.*, 2017, **139**, 10880-10886.
3. H. K. Moon, M. Son, J. E. Park, S. M. Yoon, S. H. Lee and H. C. Choi, *NPG Asia Materials*, 2012, **4**, e12-e12.
4. J. Wang, L. Liu, Q. You, Y. Song, Q. Sun, Y. Wang, Y. Cheng, F. Tan and N. Li, *Theranostics*, 2018, **8**, 955-971.
5. B.-P. Jiang, L.-F. Hu, D.-J. Wang, S.-C. Ji, X.-C. Shen and H. Liang, *J. Mater. Chem. B*, 2014, **2**, 7141-7148.
6. B. P. Jiang, L. F. Hu, X. C. Shen, S. C. Ji, Z. Shi, C. J. Liu, L. Zhang and H. Liang, *ACS Appl. Mater. Inter.*, 2014, **6**, 18008-18017.
7. Z. Wang, S. Gai, C. Wang, G. Yang, C. Zhong, Y. Dai, F. He, D. Yang and P. Yang, *Chem. Eng. J.*, 2019, **361**, 117-128.